WP15ER-PR(17) 18360

Yu A mastrikov et al.

Ab initio modelling of the initial stages of the ODS particle formation process

Preprint of Paper to be submitted for publication in
Nuclear Instruments and Methods in Physics Research
Section B

This work has been carried out within the framework of the EUROfusion Consortium and has received funding from the Euratom research and training programme 2014-2018 under grant agreement No 633053. The views and opinions expressed herein do not necessarily reflect those of the European Commission.

Ab initio modelling of the initial stages of the ODS particle formation process

Yuri A Mastrikov[1], Maxim N Sokolov[1], Sascha Koch[2], Yuri F Zhukovskii[1], Aleksejs Gopejenko[1], Pavel V Vladimirov[2], Vladimir A Borodin[3], Eugene A Kotomin[1], Anton Möslang[2]

[1]Institute of Solid State Physics, University of Latvia, Riga, Latvia
[2]Institute for Applied Materials, Karlsruhe Institute of Technology, Germany
[3]Kurchatov Institute, Moscow, Russia
yuri.mastrikov@cfi.lu.lv

Abstract. Oxide-Dispersion Strengthened (ODS) steels with Y_2O_3 nanoparticles are promising structural materials for fision and future fusion reactors. A large number of experimental as well as theoretical studies provided valuable information on the ODS particle formation process. However, some important details of this process still remain unexplained. We present the results of ab initio VASP calculations of the initial steps of the ODS particle formation . At these steps Y solute atoms are stabilized in the Fe lattice by vacancies, which create a basis for the future growth of Y_2O_3-particle. Interaction of multiple vacancies and solution Y and O atoms has been studied in various combinations and configurations.

1. Introduction

Around 1950's oxide dispersion was proposed for strengthening metallic alloys mainly with the aim of increasing their operation temperature. Since then ODS materials are being constantly improved [1]. In the 1960's the benefits of the implementation of ODS alloys as cladding materials for liquid metal fast breeder reactors were recognized [[2],[3]]. Current generation of Reduced Activation Ferritic-Martensitic steels (RAFM) strengthened by oxides allows increasing the operating temperature of and advanced fission and future fusion reactors by 100°C up to 650°C or even higher [[4],[5]]. The most commonly used oxide for the strengthening of RAFM steels is Y_2O_3. This is one of the most stable oxides with melting temperature higher than that of the steels, which makes possible the presence of the oxide in steels in a form of nanoparticles. ODS steels are produced by mechanical alloying of a mixture of steel and oxide powders for several tens of hours, followed by a hot isostatic pressing (hipping) at the temperatures around 1000-1200°C and the pressure ~100 MPa. Atomic Tomography Probe experiments reveal that solute Y and O atoms are present in steel matrix with concentrations above their equilibrium solubility [[5],[6]]. Such a supersaturation provides a basis for precipitation of Y_2O_3 nanoparticles already during the hipping stage.

Microstructure of ODS steels changes under irradiation, high operating temperatures and external stresses, which may degrade their mechanical stability [[7]-[9]]. Mechanical properties, aging and

radiation resistance of ODS steels are strongly affected by size and spatial distribution of ODS particles.

Depending on the concentration of Cr, steel may undergo $\alpha-\gamma$ phase transformation. Therefore, to cover both ferritic-martensitic (Cr < 10wt%) and ferritic steels (12-15wt% Cr) the process of ODS particle formation needs to be studied in both alpha and gamma phases [10].

In the present study we focus on interactions between single defects and their clusters in alpha-Fe. These interactions are important for understanding the variety of shape and size of ODS particles.
The main problems of the process under study are Y solute stabilization and formation of the Y-O bonds in the iron matrix. There is a strong repulsion between Y solute atoms and the atoms of the iron lattice. Due to the big mismatch between the Y_2O_3-bixbyite type structure and the *bcc* Fe, Y solute atoms have to be stabilized in the host matrix by vacancies. Vacancies play an essential role in Y precipitation process as well as in formation of Y-O bonds.

2. Model and Method

We propose a two-step theoretical approach for the atomistic simulation of the oxide nanoparticle formation. The first step, described in the present work, is extensive *ab initio* calculations of various defect complexes (vacancies, yttrium and oxygen atoms) in different configurations, using the computer code VASP 5.3 [11]. Defect interaction energies and migration barriers of atoms from these calculations, supposed to be used by a lattice kinetic Monte Carlo (LKMC) model. This approach allows us to increase the number of atoms up to several hundreds and realistically simulate the process under study. Efficiency of such an approach was already proven for similar systems [12].
For most of the simulations a cubic supercell with the extensions of $4a_0\times4a_0\times4a_0$ was used. It provides the lowest number of atoms for speeding up the calculations in a combination with the largest distance along the direction of the strongest interaction in *bcc* lattice - <111>. Core electrons are represented by the PAW-PBE [[13],[14]] potentials (see Table 1 in SMError: Reference source not found). Brillouin zone is sampled using the 4×4×4 k-point mesh, generated according to the Monkhorst-Pack scheme [15]. After performing test calculations, the plain-waive basis set kinetic energy cutoff was selected to be 450eV as a tradeoff between sufficient accuracy and calculation speed. Lattice parameters are optimized for the ideal lattice and kept fixed for all calculations with defects. For each configuration atomic positions are optimized by minimization of the total energy. Test calculations for different magnetic states showed that the largest difference in energies is between diamagnetic state and all other magnetic states. Since the difference within the magnetic states was negligible, for our model we chose ferromagnetic state as the most stable one. Interaction energies are calculated with respect to isolated single defects: V_{Fe}, Y_{Fe}, O_{8c} (global reference Error: Reference source not found), as well as with respect to isolated complexes of defects (local referenceError: Reference source not found).

$$E_{global}=E_{sys}+E_{ideal}\left(N-n_{Fe}+n_O-1\right)-\left(E_{vac}\left(N-n_{Fe}-n_Y\right)+E_Y n_Y+E_O n_O\right) \quad \text{Eq. 1}$$

, where E_{sys} - energy of the supercell with defects, E_{ideal}- energy of the ideal Fe supercell, E_{vac}, E_Y, E_O – energies of the supercells with a single V_{Fe}, Y_{Fe}, O_{8c}, respectively, N-number of atoms in the ideal supercell, n – number of Fe, Y and O atoms in supercell.

$$E_{local}=E_{sysAB}+E_{ideal}-\left(E_{sysA}+E_{sysB}\right) \quad \text{Eq. 2}$$

,where E_{sysAB}-energy of the supercell with interacting *A* and *B* complexes, E_{sysA} and E_{sysB} – energies of supercells with isolated *A* and *B* complexes. *A* and/or *B* may represent single defects as well. In case if both *A* and *B* systems are single defects, E_{local} becomes equal E_{global}.

For calculations of the Minimal Energy Path (MEP) the climbing image Nudged Elastic Band (cNEB) method [[16],[17]] was applied.

The computer code VASP was validated on examples of single point defects: monovacancy V_{Fe}, substitutional solute yttrium atom Y_{Fe}, and interstitial oxygen O_{int}. Hereafter a subscript after element name is denoting whether this specie is positioned on the regular iron lattice site (Fe), or interstitial

position, which might be further detailed in terms of Wyckoff positions (Table 2 in SM). The results for single defects are summarized in Table 3 in SMError: Reference source not found. The lowest energy configuration for yttrium is in the middle between two vacancies on the nearest neighbour sites of *bcc* iron lattice, while oxygen solute is stable at the octahedral interstitial position. To be able to map such configurations to the ridged lattice used in kinetic Monte Carlo code, one has to extend the ideal bcc iron lattice (Wyckoff symbol 2*a* for the regular Fe-lattice site) with 8*c*, 6*b* and 12d Wyckoff positions, corresponding to the middle of the shortest 2*a*-2*a* bond, octahedral and tetrahedral interstitial positions within *bcc* Fe-lattice, respectively.

Each combination of defects is uniquely described by a distance matrix given in terms of Nearest Neighbours (NN). It should be noted that in this paper, the NN index is given with respect to either iron lattice (denoted 2*a*-2*a* or omitted) or extended lattice (denoted as NN(*x*-*y*), where *x*,*y* = 2*a*, 8*c*, 6*b*, 12*d*). An example is given in Table 4 in SMError: Reference source not found.

Calculated monovacancy formation energy of 2.16 eV is slightly overestimated with respect to the experimental value, which is in line with other theoretical studies [18]. Vacancy migration was modelled along the <111> and <100> directions with the activation barriers of 0.7(0.67[20], 0.65[21]) and 2.6 eV, respectively (Figure 1).

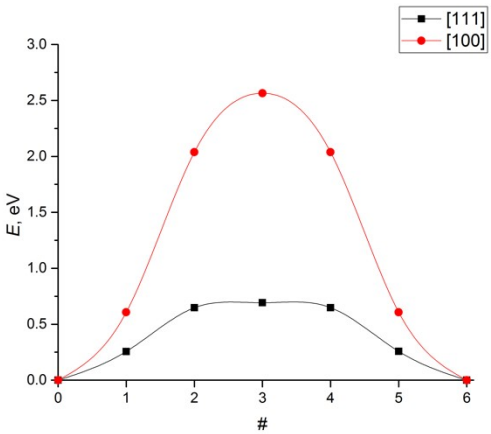

Figure 1. Barriers for vacancy jumps in the <111> and <100> direction. Energy is given relatively to stable configuration. On horizontal axis the number of NEB image is marked.

Y solute may be found in the host lattice as substitute, close to or at 8*c* site, between two adjacent vacancies along the <111>. Oversized with respect to iron matrix Y solute requires vacancies for stabilization in the bcc lattice, as well as for migration in it, which is discussed below.

Pair-wise interactions were calculated as a combination of V_{Fe}, Y_{Fe} and octahedral O_{6b} Y_{Fe}-O_{6b} (2*a*-6*b*) interaction was discarded since Y solute has to be stabilized by vacancies, before creation of the Y-O bond. Below we consider interaction of Y and O single solutes, with the former stabilized within vacancy clustersError: Reference source not found.

Detailed analysis of the interaction between two vacancies revealed the strongest attraction at the 2NN -0.23ev, and slightly smaller at the 1NN -0.14eV. Beyond the 3NN, the interaction is lower than 0.05eV and can be disregarded (Table 5 in SMError: Reference source not found).

Calculations of the pairwise Y_{Fe}-Y_{Fe} interaction (Table 5 in SMError: Reference source not found) showed a weak attraction of ~0.1eV at the 2NN and the 3NN. At the 5NN, along the <111>, interaction of 0.2eV is repulsive. Other interaction energies at close distances are negligibly small.

There are two stable interstitial positions for oxygen in the *bcc* Fe lattice: 6*b* (octahedral) and 12*d* (tetrahedral) - Figure 2.

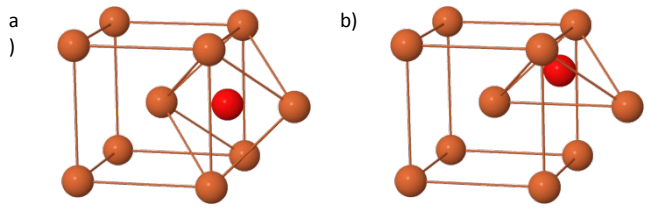

Figure 2. Oxygen in the *bcc* Fe lattice at interstitial octahedral 6*b* a) and tetrahedral 12*d* b) positions.

The former is more energetically favorable by 0.5eV. The interaction between two oxygen atoms at octahedral positions is repulsive. The strongest repulsion has been observed for the 4NN (6*b*-6*b*Error: Reference source not found).

Oxygen solute occupies interstitial 6*b* sites, unless 2*a* site is available (Table 5 in SMError: Reference source not found). The solute migrates from one 6*b* to another 6*b*, via 12*d* site with the activation energy practically equal to the difference between these two states - 0.52 eV (Figure 3) (0.48eV [21]).

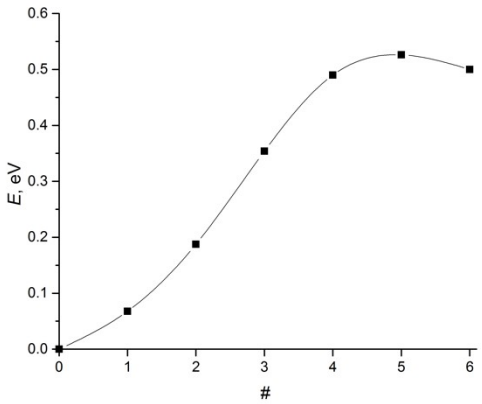

Figure 3. Barrier for transition between O at 6*b* and the nearest to it O at 12*d* site. O_{6b} energy is taken as a reference. On horizontal axis the number of NEB image is marked.

3. Results

Yttrium atom is oversized with respect to the iron matrix, so its introduction even into substitutional position creates local compressive stresses around it which can be reduced substantially by introduction of vacancies.

Our calculations show that vacancies in the *bcc* iron lattice tend to accumulate, forming stable clusters (Table 6 in SMError: Reference source not found). Vacancy cluster size has been varied from one to nine vacancies. Binding energies were calculated with respect to complete cluster dissolution into isolated vacancies using:

$$E_{bindN} = E_{clusterN} + (N-1)\,E_{bulk} - N\,E_{single\ vac} \qquad \text{Eq. 3}$$

The growth of vacancy cluster in the *bcc* iron lattice is energetically favourable. For clusters with more than two vacancies the most stable configuration corresponds to the smallest mutual distances between the defects.

Stabilization of Y solute requires more than one vacancy per one solute Y atom. Y_{Fe} solute creates a large local stress. Vacancy, placed right next to it, makes the solute change its position from the regular Fe-lattice site (2*a*) to the middle of 1NN bond (8*c*), creating configuration Table 8Error: Reference source not found(a) in SM.

Migration of Y solute is a vacancy-assisted two-step process. First, jumps adjacent vacancy (Fe atom), then – Y solute. Y-V_{Fe} complex has several stable configurations Table 8 Error: Reference source not found(a-c) in SM.

In all transitions, except theError: Reference source not found b) - b), Y solute remains at the same site. Actual migration of Y solute occurs only along the <100> with a relatively low activation barrier of 0.45eV. The a) - b) transition is, however, the migration rate determining step.

The most energetically favourable configurations for single Y solute and multiple vacancies are shown in Table 8 in SMError: Reference source not found. Binding energy was calculated with respect to complete cluster decomposition into isolated vacancies and isolated Y_{Fe} (Error: Reference source not found).

$$E_{bindN} = E_{clusterN} + N\,E_{bulk} - N\,E_{single\,vac} - E_{single\,Y_{Fe}} \qquad \text{Eq. 4}$$

All Y/nV_{Fe} complexes are energetically stable. The complex of Y_{Fe} atom and seven vacancies (see Table 8Error: Reference source not found (r)) is stable, however the binding energy for this configuration (-5.58eV) is smaller, than that for the cluster of six (Table 8Error: Reference source not found(o) in SM) (-7.39eV) and eight (Error: Reference source not foundTable 8 (t) in SM) (-7.96eV) vacancies with Y_{6b}. Adding one more vacancy reduces the binding energy to (Error: Reference source not foundTable 8 (v) in SM) -7.12eV, which makes $Y_{6b}/6V_{Fe}$ (Error: Reference source not foundTable 8 (o) in SM) and $Y_{6b}/8V_{Fe}$ (Error: Reference source not foundTable 8 (t) in SM) clusters the most stable combinations with small number of vacancies.

Stabilized by vacancies, Y_{Fe} solute complex V_{Fe}-Y_{8c}-V_{Fe} may interact with other Y_{Fe} solute atoms. This type of interaction is modelled by varying the distance between these two defects (Table 9 in SMError: Reference source not found). As a reference the energy of isolated Y_{Fe} and V_{Fe}-Y_{8c}-V_{Fe} is taken.

At the distances between Y_{Fe} and Y_{8c} of the 3NN (2*a*-8*c*) and smaller, Y_{Fe} transforms V_{Fe}-Y_{8c}-V_{Fe} into Y_{Fe}-V_{Fe}-Y_{Fe} complex (Error: Reference source not foundTable 9(a-d) in SM). The strongest attraction has been observed for the defect aligned along the <111> direction (Error: Reference source not foundTable 9(d) in SM). For clearly separated complexes (see Table 9Error: Reference source not found(e-h) in SM) the interaction becomes weaker and does not exceed 0.15 eV.

Migrating in the host matrix, as described in Table 7 in SMError: Reference source not found, V_{Fe}-Y_{8c}-V_{Fe} complexes form 2Y/nV_{Fe} clusters. Interaction between two V_{Fe}-Y_{8c}-V_{Fe} complexes is attractive. At three closest distances, *without overlapping vacancies*, binding energy between the complexes is between 0.8-1.4eV Table 10Error: Reference source not found(b-d) in SM.

Clusters of single or multiple Y solutes, stabilized by vacancies, interact with interstitial and substitutional O solutes, creating the very initial building blocks for the Y/O nanoparticle. Our calculation of single Y and O solutes showed attraction at all distances. The strongest attraction energy corresponds to the configuration Error: Reference source not foundTable 11(b) in SM.

4. Summary

Our calculations have confirmed the applicability of the DFT method, as implemented in the computer code VASP. The following conclusions can be drawn:Vacancies precipitate, creating stable clusters in the *bcc* Fe lattice. Y solute atoms can be stabilized in the host matrix by vacancies. Y solute migration occurs in multiple steps by the vacancy mechanism. Clusters with 2 and 1.5 vacancies per Y solute atom provide a basis for creation Y-O-bixbyite type bonds.

5. Acknowledgements

This work has been carried out within the framework of the EUROfusion Consortium and has received funding from the Euratom research and training programme 2014-2018 under grant agreement No 633053. The views and opinions expressed herein do not necessarily reflect those of the European Commission.

References

[1] C. Cayron, E. Rath, S. Launois, Journal of Nuclear Materials **335** (2004) 83–102

[2] R. Lindau, A. Möslang, M. Schirra, P. Schlossmacher, M. Klimenkov, Journal of Nuclear Materials **307–311** (2002) 769–772

[3] Chenwei He. Experimental study of the interaction of vacancy defects with Y, O and Ti solutes to better understand their roles in the nanoparticles formation in ODS steels. Materials. Universite d'Orleans, 2014. English. <NNT : 2014ORLE2057>. <tel-01207172>

[4] M. Klimiankou, R. Lindau, and A. Möslang, J. Nucl. Materials **367–370** (2007) 173–178

[5] T. Okuda and M. Fujiwara, J. Mater. Sci. Lett. **14** (1995), 1600-1603.

[6] G.R. Odette, M.J. Alinger, and B.D. Wirth, Ann. Rev. Mater. Research **38** (2008) 471-503.

[7] Ya. Zhang et al., Nuclear Instruments and Methods in Physics Research B **297** (2013) 35–38

[8] S. Sojak et al., Nuclear Instruments and Methods in Physics Research B **365** (2015) 305–308

[9] Yo. Ha et al., Nuclear Instruments and Methods in Physics Research B **365** (2015) 313–318

[10] A. Gopejenko, Yu. F. Zhukovskii, E. A. Kotomin, Phusica Status Solidi B, **253**, 11, 2136-2143 (2016)

[11] G. Kresse and J. Hafner, Phys. Rev. B **47** , 558 (1993); ibid. **49** , 14 251 (1994)

[12] V.A. Borodin et al., Journal of Nuclear Materials **367–370** (2007) 286–291

[13] P.E. Blöchl, Phys. Rev. B **50**, 17953 (1994).

[14] G. Kresse, and J. Joubert, Phys. Rev. B **59**, 1758 (1999)

[15] H. J. Monkhorst and J. D. Pack, Phys. Rev. B **13**, 5188 (1976)

[16] G. Henkelman and H. Jónsson, J. Chem. Phys. **113**, 9901-9904 (2000)

[17] G. Henkelman and H. Jónsson, J. Chem. Phys. **113**, 9978-9985 (2000)

[18] P. Olsson et al., Rev. B **75**, 014110 (2007).

[19] P. Söderlind et al., Physical Review B **61**, 2579-2586 (2000)

[20] C.-C. Fu et al., Nature materials, (2005) **4**, 68.

[21] A. Claisse, P. Olsson / Nuclear Instruments and Methods in Physics Research B **303** (2013) 18–22

[22] C.S. Becquart, C. Domain / Nucl. Instr. and Meth. in Phys. Res. B **202** (2003) 44–50

[23] A. Claisse, Ab initio based multi-scale simulations of oxide dispersion strengthened steels, KTH, 2012

[24] D. Murali et al. / Journal of Nuclear Materials **419** (2011) 208–212

[25] D. Murali, B.K. Panigrahi, M.C. Valsakumar, Sharat Chandra, C.S. Sundar, and Baldev Raj, Journal of Nuclear Materials, **403**:113-116, 2010.

Supplementary Materials

Table 1 Core PAW PBE potentials.

core potential for	valence electrons	cutoff energy, eV
Fe	$3d^6 4s^2$	267.883
Y	$4s^2 4p^6 4d^1 5s^2$	211.641
O	$2s^2 2p^4$	400.000

Table 2. Wyckoff Positions of Group 229 (*Im-3m*)

Multiplicity	Wyckoff letter	Site symmetry	Coordinates	
2	*a*	m-3m	(0, 0, 0)	
6	*b*	4/mm. m	(0,1/2,1/2) (1/2,0,1/2) (1/2,1/2,0)	
8	*c*	.-3m	(1/4,1/4,1/4) (3/4,3/4,1/4) (3/4,1/4,3/4) (1/4,3/4,3/4)	
12	*d*	-4m. 2	(1/4,0,1/2) (3/4,0,1/2) (1/2,1/4,0) (1/2,3/4,0) (0,1/2,1/4) (0,1/2,3/4)	

Table 3. Single defects energies (eV), formation for V_{Fe} and self-interstitials, binding between Y_{Fe} and O_{Fe} solutes and V_{Fe}. Higher values correspond to less favourable states.

		defect			
site	Comment	V_{Fe}	Fe	Y	O
2*a*	regular Fe lattice site	2.16(2.15[1])	0	ref. state	ref. state
8*c*	middle between 1NN regular sites			-1.35*	3.01
6*b*	octahedral		5.31(5.29[1])	15.06	0.51
12*d*	tetrahedral		4.40(4.44[1])	8.40	1.01
dumbbell <100>			5.19(5.13[1])		
dumbbell <110>			4.05(4.02[1])		
dumbbell <111>			4.78(4.72[1])		

[1][18]

*Configuration as in Error: Reference source not found.

Table 4. The ground state configuration of Y solute located at 8*c* site between two nearest V_{Fe}.

	Y_{8c}	V_{Fe}	V_{Fe}
Y_{8c}	0	1(2*a*-8*c*)	1(2*a*-8*c*)
V_{Fe}		0	1(2*a*-2*a*)
V_{Fe}			0

Table 5. Pair-wise interaction of V_{Fe}, Y_{Fe} and O_{6b}.

	Self-interaction				
	V_{Fe}(2*a*-2*a*)	Y_{Fe}(2*a*-2*a*)	O_{6b}(6*b*-6*b*)	V_{Fe}-Y_{Fe}(2*a*-2*a*)	V_{Fe}-O_{6b}(2*a*-6*b*)
0				unstable	-0.58
1	-0.14(-0.14[1])	0.02(0.04[2])	0.70(0.73[3])	-1.35*(-1.27[2,3],-1.45[4])	-1.63(-1.69[3],-1.65[5])
2	-0.23(-0.28[1])	-0.12(-0.06[2])	0.49(0.46[3])	-0.20(-0.20[2,3],-0.26[4])	-0.69(-0.73[3],-0.75[5])
3	0.01(0.02[1])	-0.10(-0.08[2])	0.00(0.11[3])	-0.12(-0.13[2,3],-0.24[4])	-0.11(-0.14[3])
4	-0.05	0.00(0.04[2])	1.81(1.59/-0.13[3])	-0.06(-0.04[2,3],-0.15[4])	-0.34(-0.37[3])
5	-0.06	0.12(0.11[2])	0.27(0.23[3])	-0.19(-0.20[2,3],-0.25[4])	0.12(-0.01[3])
6	-0.02	-0.02	0.17(0.12[3])	-0.07	0.03

*Stable as the configuration in Error: Reference source not found

[1][22]
[2][21]
[3][23]
[4][24]
[5][25]

Table 6 Binding energies between multiple vacancies.

	vacancy cluster size	configuration	binding energy, eV
a)	1	V_{Fe} V_{Fe} 0	0.00
b)	2	V_{Fe} V_{Fe} V_{Fe} 0 2(2*a*-2*a*) V_{Fe} 0	-0.23(-0.28[1])
c)	3	V_{Fe} V_{Fe} V_{Fe} V_{Fe} 0 1(2*a*-2*a*) 1(2*a*-2*a*) V_{Fe} 0 2(2*a*-2*a*) V_{Fe} 0	-0.65(-0.64[1])
d)	4	V_{Fe} V_{Fe} V_{Fe} V_{Fe} V_{Fe} 0 1(2*a*-2*a*) 1(2*a*-2*a*) 2(2*a*-2*a*) V_{Fe} 0 2(2*a*-2*a*) 1(2*a*-2*a*) V_{Fe} 0 1(2*a*-2*a*) V_{Fe} 0	-1.38(-1.34[1])
e)	5	V_{Fe} V_{Fe} V_{Fe} V_{Fe} V_{Fe} V_{Fe} 0 1(2*a*-2*a*) 2(2*a*-2*a*) 1(2*a*-2*a*) 3(2*a*-2*a*) V_{Fe} 0 1(2*a*-2*a*) 2(2*a*-2*a*) 1(2*a*-2*a*) V_{Fe} 0 1(2*a*-2*a*) 2(2*a*-2*a*)	-2.19

		V_{Fe}				0	1(2*a*-2*a*)					
		V_{Fe}					0					
f)			V_{Fe}	V_{Fe}	V_{Fe}	V_{Fe}	V_{Fe}	V_{Fe}				
		V_{Fe}	0	1(2*a*-2*a*)	1(2*a*-2*a*)	1(2*a*-2*a*)	1(2*a*-2*a*)	2(2*a*-2*a*)				
		V_{Fe}		0	2(2*a*-2*a*)	2(2*a*-2*a*)	3(2*a*-2*a*)	1(2*a*-2*a*)				
	6	V_{Fe}			0	3(2*a*-2*a*)	2(2*a*-2*a*)	1(2*a*-2*a*)				-3.18
		V_{Fe}				0	2(2*a*-2*a*)	1(2*a*-2*a*)				
		V_{Fe}					0	1(2*a*-2*a*)				
		V_{Fe}						0				
g)			V_{Fe}	V_{Fe}	V_{Fe}	V_{Fe}	V_{Fe}	V_{Fe}	V_{Fe}			
		V_{Fe}	0	2(2*a*-2*a*)	3(2*a*-2*a*)	1(2*a*-2*a*)	2(2*a*-2*a*)	3(2*a*-2*a*)	5(2*a*-2*a*)			
		V_{Fe}		0	2(2*a*-2*a*)	1(2*a*-2*a*)	3(2*a*-2*a*)	5(2*a*-2*a*)	3(2*a*-2*a*)			
		V_{Fe}			0	1(2*a*-2*a*)	5(2*a*-2*a*)	3(2*a*-2*a*)	2(2*a*-2*a*)			
	7	V_{Fe}				0	1(2*a*-2*a*)	1(2*a*-2*a*)	1(2*a*-2*a*)			-2.94
		V_{Fe}					0	2(2*a*-2*a*)	3(2*a*-2*a*)			
		V_{Fe}						0	2(2*a*-2*a*)			
		V_{Fe}							0			
h)			V_{Fe}	V_{Fe}	V_{Fe}	V_{Fe}	V_{Fe}	V_{Fe}	V_{Fe}			
		V_{Fe}	0	1(2*a*-2*a*)	1(2*a*-2*a*)	1(2*a*-2*a*)	1(2*a*-2*a*)	1(2*a*-2*a*)	1(2*a*-2*a*)			
		V_{Fe}		0	2(2*a*-2*a*)	2(2*a*-2*a*)	3(2*a*-2*a*)	3(2*a*-2*a*)	5(2*a*-2*a*)			
		V_{Fe}			0	3(2*a*-2*a*)	2(2*a*-2*a*)	5(2*a*-2*a*)	3(2*a*-2*a*)			
	7	V_{Fe}				0	2(2*a*-2*a*)	2(2*a*-2*a*)	3(2*a*-2*a*)			-3.32
		V_{Fe}					0	3(2*a*-2*a*)	2(2*a*-2*a*)			
		V_{Fe}						0	2(2*a*-2*a*)			
		V_{Fe}							0			
i)			V_{Fe}	V_{Fe}	V_{Fe}	V_{Fe}	V_{Fe}	V_{Fe}	V_{Fe}	V_{Fe}		
		V_{Fe}	0	2(2*a*-2*a*)	3(2*a*-2*a*)	1(2*a*-2*a*)	4(2*a*-2*a*)	3(2*a*-2*a*)	5(2*a*-2*a*)	9(2*a*-2*a*)		
		V_{Fe}		0	2(2*a*-2*a*)	1(2*a*-2*a*)	1(2*a*-2*a*)	2(2*a*-2*a*)	3(2*a*-2*a*)	5(2*a*-2*a*)		
		V_{Fe}			0	1(2*a*-2*a*)	1(2*a*-2*a*)	3(2*a*-2*a*)	2(2*a*-2*a*)	3(2*a*-2*a*)		
	8	V_{Fe}				0	2(2*a*-2*a*)	1(2*a*-2*a*)	1(2*a*-2*a*)	4(2*a*-2*a*)		-4.23
		V_{Fe}					0	1(2*a*-2*a*)	1(2*a*-2*a*)	1(2*a*-2*a*)		
		V_{Fe}						0	2(2*a*-2*a*)	3(2*a*-2*a*)		
		V_{Fe}							0	2(2*a*-2*a*)		
		V_{Fe}								0		
j)			V_{Fe}	V_{Fe}	V_{Fe}	V_{Fe}	V_{Fe}	V_{Fe}	V_{Fe}	V_{Fe}	V_{Fe}	
		V_{Fe}	0	2(2*a*-2*a*)	2(2*a*-2*a*)	3(2*a*-2*a*)	1(2*a*-2*a*)	2(2*a*-2*a*)	3(2*a*-2*a*)	3(2*a*-2*a*)	5(2*a*-2*a*)	
		V_{Fe}		0	3	2(2*a*-2*a*)	1(2*a*-2*a*)	3(2*a*-2*a*)	2(2*a*-2*a*)	5(2*a*-2*a*)	3(2*a*-2*a*)	
		V_{Fe}			0	2(2*a*-2*a*)	1(2*a*-2*a*)	3(2*a*-2*a*)	5(2*a*-2*a*)	2(2*a*-2*a*)	3(2*a*-2*a*)	
		V_{Fe}				0	1(2*a*-2*a*)	5(2*a*-2*a*)	3(2*a*-2*a*)	3(2*a*-2*a*)	2(2*a*-2*a*)	
	9	V_{Fe}					0	1(2*a*-2*a*)	1(2*a*-2*a*)	1(2*a*-2*a*)	1(2*a*-2*a*)	-5.34
		V_{Fe}						0	2(2*a*-2*a*)	2(2*a*-2*a*)	3(2*a*-2*a*)	
		V_{Fe}							0	3(2*a*-2*a*)	2(2*a*-2*a*)	
		V_{Fe}								0	2(2*a*-2*a*)	
		V_{Fe}									0	

[1][21]

Table **7**. Stable states and migration barriers between them for the Y/V_{Fe} complex.
[1][24]

State (Table 8Error: Reference source not found)		migration energy, eV
a)	a)	3.5
b)	b)	0.45
a)	b)	2.2(2.05[1])
a)	c)	1.4(1.33[1])

Table 8. Binding energies of single solute Y atom and cluster of vacancies.

	Configuration	Binding energy, eV
a)	Y_{8c} V_{Fe} V_{Fe} Y_{8c} 0 1(2*a*-8*c*) 1(2*a*-8*c*) V_{Fe} 0 1(2*a*-2*a*) V_{Fe} 0	-1.35
b)	Y_{Fe} V_{Fe} V_{Fe} Y_{Fe} 0 2(2*a*-2*a*) V_{Fe} 0	-0.19
c)	Y_{Fe} V_{Fe} V_{Fe} Y_{Fe} 0 3(2*a*-2*a*) V_{Fe} 0	-0.11
d)	Y_{Fe} V_{Fe} V_{Fe} Y_{Fe} 0 1(2*a*-2*a*) 1(2*a*-2*a*) V_{Fe} 0 2(2*a*-2*a*) V_{Fe} 0	-2.89
e)	Y_{Fe} V_{Fe} V_{Fe} Y_{Fe} 0 2(2*a*-2*a*) 2(2*a*-2*a*) V_{Fe} 0 3(2*a*-2*a*) V_{Fe} 0	-0.30
f)	Y_{Fe} V_{Fe} V_{Fe} Y_{Fe} 0 1(2*a*-2*a*) 1(2*a*-2*a*) V_{Fe} 0 3(2*a*-2*a*) V_{Fe} 0	-1.37
g)	Y_{Fe} V_{Fe} V_{Fe} Y_{Fe} 0 1(2*a*-2*a*) 1(2*a*-2*a*) V_{Fe} 0 5(2*a*-2*a*) V_{Fe} 0	-1.51
h)	Y_{12d} V_{Fe} V_{Fe} V_{Fe} V_{Fe} Y_{12} 0 1(2*a*-12d) 1(2*a*-12d) 1(2*a*-12d) 1(2*a*-12d)	-4.89

d						
V_{Fe}		0	2(2a-2a)	1(2a-2a)	1(2a-2a)	
V_{Fe}			0	1(2a-2a)	1(2a-2a)	
V_{Fe}				0	2(2a-2a)	
V_{Fe}					0	

i) -3.62

	Y_{Fe}	V_{Fe}	V_{Fe}	V_{Fe}
Y_{Fe}	0	1(2a-2a)	1(2a-2a)	1(2a-2a)
V_{Fe}		0	2(2a-2a)	3(2a-2a)
V_{Fe}			0	2(2a-2a)
V_{Fe}				0

j) -2.92

	Y_{Fe}	V_{Fe}	V_{Fe}	V_{Fe}
Y_{Fe}	0	1(2a-2a)	1(2a-2a)	1(2a-2a)
V_{Fe}		0	2(2a-2a)	3(2a-2a)
V_{Fe}			0	5(2a-2a)
V_{Fe}				0

k) -3.95

	Y_{6b}	V_{Fe}	V_{Fe}	V_{Fe}	V_{Fe}
Y_{6b}	0	2(2a-6b)	1(2a-6b)	1(2a-6b)	2(2a-6b)
V_{Fe}		0	1(2a-2a)	1(2a-2a)	3(2a-2a)
V_{Fe}			0	2(2a-2a)	1(2a-2a)
V_{Fe}				0	1(2a-2a)
V_{Fe}					0

l) -6.02

	Y_{6b}	V_{Fe}	V_{Fe}	V_{Fe}	V_{Fe}	V_{Fe}
Y_{6b}	0	2(2a-6b)	2(2a-6b)	1(2a-6b)	1(2a-6b)	2(2a-6b)
V_{Fe}		0	2(2a-2a)	1(2a-2a)	1(2a-2a)	2(2a-2a)
V_{Fe}			0	1(2a-2a)	1(2a-2a)	3(2a-2a)
V_{Fe}				0	2(2a-2a)	1(2a-2a)
V_{Fe}					0	1(2a-2a)
V_{Fe}						0

m) -3.13

	Y_{Fe}	V_{Fe}	V_{Fe}	V_{Fe}	V_{Fe}
Y_{Fe}	0	1(2a-2a)	1(2a-2a)	1(2a-2a)	1(2a-2a)
V_{Fe}		0	3(2a-2a)	2(2a-2a)	5(2a-2a)
V_{Fe}			0	5(2a-2a)	2(2a-2a)
V_{Fe}				0	3(2a-2a)
V_{Fe}					0

n) -4.61

	Y_{Fe}	V_{Fe}	V_{Fe}	V_{Fe}	V_{Fe}
Y_{Fe}	0	1(2a-2a)	1(2a-2a)	1(2a-2a)	1(2a-2a)
V_{Fe}		0	2(2a-2a)	2(2a-2a)	3(2a-2a)
V_{Fe}			0	3(2a-2a)	2(2a-2a)
V_{Fe}				0	2(2a-2a)
V_{Fe}					0

o) -7.39

		Y_{6b}	V_{Fe}	V_{Fe}	V_{Fe}	V_{Fe}	V_{Fe}	V_{Fe}
Y_{6b}		0	1(2a-6b)	2(2a-6b)	2(2a-6b)	2(2a-6b)	2(2a-6b)	1(2a-6b)
V_{Fe}			0	1(2a-2a)	1(2a-2a)	1(2a-2a)	1(2a-2a)	2(2a-2a)

V_{Fe}			0	2(2*a*-2*a*)	2(2*a*-2*a*)	3(2*a*-2*a*)	1(2*a*-2*a*)
V_{Fe}				0	3(2*a*-2*a*)	2(2*a*-2*a*)	1(2*a*-2*a*)
V_{Fe}					0	2(2*a*-2*a*)	1(2*a*-2*a*)
V_{Fe}						0	1(2*a*-2*a*)
V_{Fe}							0

p) -4.95

	Y_{Fe}	V_{Fe}	V_{Fe}	V_{Fe}	V_{Fe}	V_{Fe}
Y_{Fe}	0	1(2*a*-2*a*)	1(2*a*-2*a*)	1(2*a*-2*a*)	1(2*a*-2*a*)	1(2*a*-2*a*)
V_{Fe}		0	2(2*a*-2*a*)	2(2*a*-2*a*)	3(2*a*-2*a*)	2(2*a*-2*a*)
V_{Fe}			0	3(2*a*-2*a*)	2(2*a*-2*a*)	3(2*a*-2*a*)
V_{Fe}				0	2(2*a*-2*a*)	3(2*a*-2*a*)
V_{Fe}					0	5(2*a*-2*a*)
V_{Fe}						0

q) -4.94

	Y_{Fe}	V_{Fe}	V_{Fe}	V_{Fe}	V_{Fe}	V_{Fe}	V_{Fe}
Y_{Fe}	0	1(2*a*-2*a*)	1(2*a*-2*a*)	1(2*a*-2*a*)	1(2*a*-2*a*)	1(2*a*-2*a*)	1(2*a*-2*a*)
V_{Fe}		0	3(2*a*-2*a*)	2(2*a*-2*a*)	3(2*a*-2*a*)	2(2*a*-2*a*)	5(2*a*-2*a*)
V_{Fe}			0	2(2*a*-2*a*)	3(2*a*-2*a*)	5(2*a*-2*a*)	2(2*a*-2*a*)
V_{Fe}				0	5(2*a*-2*a*)	3(2*a*-2*a*)	3(2*a*-2*a*)
V_{Fe}					0	2(2*a*-2*a*)	2(2*a*-2*a*)
V_{Fe}						0	3(2*a*-2*a*)
V_{Fe}							0

r) -5.58

	Y_{Fe}	V_{Fe}	V_{Fe}	V_{Fe}	V_{Fe}	V_{Fe}	V_{Fe}
Y_{Fe}	0	1(2*a*-2*a*)	1(2*a*-2*a*)	1(2*a*-2*a*)	1(2*a*-2*a*)	1(2*a*-2*a*)	1(2*a*-2*a*)
V_{Fe}		0	2(2*a*-2*a*)	2(2*a*-2*a*)	3(2*a*-2*a*)	3(2*a*-2*a*)	5(2*a*-2*a*)
V_{Fe}			0	3(2*a*-2*a*)	2(2*a*-2*a*)	5(2*a*-2*a*)	3(2*a*-2*a*)
V_{Fe}				0	2(2*a*-2*a*)	2(2*a*-2*a*)	3(2*a*-2*a*)
V_{Fe}					0	3(2*a*-2*a*)	2(2*a*-2*a*)
V_{Fe}						0	2(2*a*-2*a*)
V_{Fe}							0

s) -5.21

	Y_{Fe}	V_{Fe}	V_{Fe}	V_{Fe}	V_{Fe}	V_{Fe}	V_{Fe}
Y_{Fe}	0	1(2*a*-2*a*)	1(2*a*-2*a*)	1(2*a*-2*a*)	1(2*a*-2*a*)	1(2*a*-2*a*)	1(2*a*-2*a*)
V_{Fe}		0	3	2(2*a*-2*a*)	3(2*a*-2*a*)	2(2*a*-2*a*)	3(2*a*-2*a*)
V_{Fe}			0	2(2*a*-2*a*)	3(2*a*-2*a*)	5(2*a*-2*a*)	3(2*a*-2*a*)
V_{Fe}				0	5(2*a*-2*a*)	3(2*a*-2*a*)	2(2*a*-2*a*)
V_{Fe}					0	2(2*a*-2*a*)	3(2*a*-2*a*)
V_{Fe}						0	2(2*a*-2*a*)
V_{Fe}							0

t) -7.96

	Y_{6b}	V_{Fe}	V_{Fe}	V_{Fe}	V_{Fe}	V_{Fe}	V_{Fe}	V_{Fe}	V_{Fe}
Y_{6b}	0	1(2*a*-6*b*)	2(2*a*-6*b*)	2(2*a*-6*b*)	2(2*a*-6*b*)	2(2*a*-6*b*)	1(2*a*-6*b*)	4(2*a*-2*a*)	4(2*a*-2*a*)
V_{Fe}		0	1(2*a*-2*a*)	1(2*a*-2*a*)	1(2*a*-2*a*)	1(2*a*-2*a*)	2(2*a*-2*a*)	1(2*a*-2*a*)	4(2*a*-2*a*)
V_{Fe}			0	2(2*a*-2*a*)	2(2*a*-2*a*)	3(2*a*-2*a*)	1(2*a*-2*a*)	5(2*a*-2*a*)	2(2*a*-2*a*)
V_{Fe}				0	3(2*a*-2*a*)	2(2*a*-2*a*)	1(2*a*-2*a*)	3(2*a*-2*a*)	3(2*a*-2*a*)
V_{Fe}					0	2(2*a*-2*a*)	1(2*a*-2*a*)	3(2*a*-2*a*)	3(2*a*-2*a*)

	V_{Fe}						0	1(2*a*-2*a*)	2(2*a*-2*a*)	5(2*a*-2*a*)		
	V_{Fe}							0	4(2*a*-2*a*)	1(2*a*-2*a*)		
	V_{Fe}								0	9(2*a*-2*a*)		
	V_{Fe}									0		
u)		Y_{Fe}	V_{Fe}	V_{Fe}	V_{Fe}	V_{Fe}	V_{Fe}	V_{Fe}	V_{Fe}	V_{Fe}		-6.15
	Y_{Fe}	0	1(2*a*-2*a*)	1(2*a*-2*a*)	1(2*a*-2*a*)	1(2*a*-2*a*)	1(2*a*-2*a*)	1(2*a*-2*a*)	1(2*a*-2*a*)			
	V_{Fe}		0	2(2*a*-2*a*)	2(2*a*-2*a*)	3(2*a*-2*a*)	2(2*a*-2*a*)	3(2*a*-2*a*)	5(2*a*-2*a*)			
	V_{Fe}			0	3(2*a*-2*a*)	2(2*a*-2*a*)	3(2*a*-2*a*)	2(2*a*-2*a*)	3(2*a*-2*a*)			
	V_{Fe}				0	2(2*a*-2*a*)	3(2*a*-2*a*)	5(2*a*-2*a*)	3(2*a*-2*a*)			
	V_{Fe}					0	5(2*a*-2*a*)	3(2*a*-2*a*)	2(2*a*-2*a*)			
	V_{Fe}						0	2(2*a*-2*a*)	3(2*a*-2*a*)			
	V_{Fe}							0	2(2*a*-2*a*)			
	V_{Fe}								0			
v)		Y_{Fe}	V_{Fe}	V_{Fe}	V_{Fe}	V_{Fe}	V_{Fe}	V_{Fe}	V_{Fe}	V_{Fe}		-7.12
	Y_{Fe}	0	1(2*a*-2*a*)	1(2*a*-2*a*)	1(2*a*-2*a*)	1(2*a*-2*a*)	1(2*a*-2*a*)	1(2*a*-2*a*)	1(2*a*-2*a*)	1(2*a*-2*a*)		
	V_{Fe}		0	2(2*a*-2*a*)	2(2*a*-2*a*)	3(2*a*-2*a*)	2(2*a*-2*a*)	3(2*a*-2*a*)	3(2*a*-2*a*)	5(2*a*-2*a*)		
	V_{Fe}			0	3(2*a*-2*a*)	2(2*a*-2*a*)	3(2*a*-2*a*)	2(2*a*-2*a*)	5(2*a*-2*a*)	3(2*a*-2*a*)		
	V_{Fe}				0	2(2*a*-2*a*)	3(2*a*-2*a*)	5(2*a*-2*a*)	2(2*a*-2*a*)	3(2*a*-2*a*)		
	V_{Fe}					0	5(2*a*-2*a*)	3(2*a*-2*a*)	3(2*a*-2*a*)	2(2*a*-2*a*)		
	V_{Fe}						0	2(2*a*-2*a*)	2(2*a*-2*a*)	3(2*a*-2*a*)		
	V_{Fe}							0	3(2*a*-2*a*)	2(2*a*-2*a*)		
	V_{Fe}								0	2(2*a*-2*a*)		
	V_{Fe}									0		

Table 9. Interaction of a single solute atom Y_{Fe} with the V_{Fe}-Y_{8c}-V_{Fe} complex

	Configuration	Binding energy, eV	Configuration
a)	<table><tr><td></td><td>Y_{Fe}</td><td>Y_{Fe}</td><td>V_{Fe}</td></tr><tr><td>Y_{Fe}</td><td>0</td><td>2 (2*a*-2*a*)</td><td>1 (2*a*-2*a*)</td></tr><tr><td>Y_{Fe}</td><td></td><td>0</td><td>1 (2*a*-2*a*)</td></tr><tr><td>V_{Fe}</td><td></td><td></td><td>0</td></tr></table>	-0.30	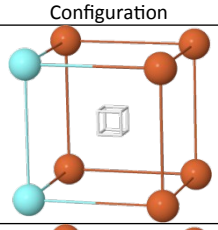
b)	<table><tr><td></td><td>Y_{Fe}</td><td>Y_{Fe}</td><td>V_{Fe}</td></tr><tr><td>Y_{Fe}</td><td>0</td><td>3 (2*a*-2*a*)</td><td>1 (2*a*-2*a*)</td></tr><tr><td>Y_{Fe}</td><td></td><td>0</td><td>1 (2*a*-2*a*)</td></tr><tr><td>V_{Fe}</td><td></td><td></td><td>0</td></tr></table>	-1.03	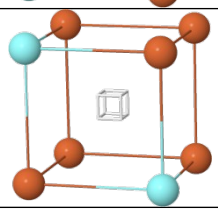

c)

	Y_{Fe}	Y_{Fe}	V_{Fe}
Y_{Fe}	0	4 (2*a*-2*a*)	1 (2*a*-2*a*)
Y_{Fe}		0	2 (2*a*-2*a*)
V_{Fe}			0

-0.27

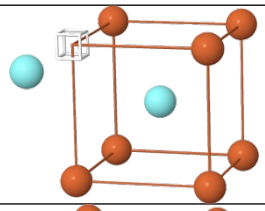

d)

	Y_{Fe}	Y_{Fe}	V_{Fe}
Y_{Fe}	0	5 (2*a*-2*a*)	1 (2*a*-2*a*)
Y_{Fe}		0	1 (2*a*-2*a*)
V_{Fe}			0

-1.16

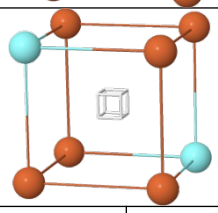

e)

	Y_{Fe}	Y_{6b}	V_{Fe}	V_{Fe}
Y_{Fe}	0	5(2*a*-6*b*)	3(2*a*-6*a*)	4(2*a*-6*a*)
Y_{6b}		0	1(2*a*-6*b*)	1(2*a*-6*b*)
V_{Fe}			0	1 (2*a*-2*a*)
V_{Fe}				0

-0.01

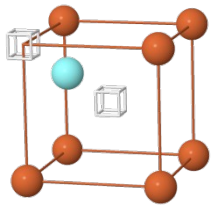

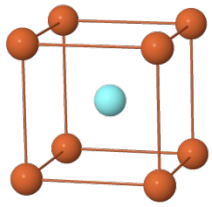

f)

	Y_{Fe}	Y_{6b}	V_{Fe}	V_{Fe}
Y_{Fe}	0	6(2*a*-6*b*)	4(2*a*-6*a*)	5(2*a*-6*a*)
Y_{6b}		0	1(2*a*-6*b*)	1(2*a*-6*b*)
V_{Fe}			0	1 (2*a*-2*a*)
V_{Fe}				0

0.13

g)

	Y_{Fe}	Y_{6b}	V_{Fe}	V_{Fe}
Y_{Fe}	0	7(2*a*-6*b*)	4(2*a*-6*a*)	6(2*a*-6*a*)
Y_{6b}		0	1(2*a*-6*b*)	1(2*a*-6*b*)
V_{Fe}			0	1 (2*a*-2*a*)
V_{Fe}				0

0.04

h)

	Y_{Fe}	Y_{6b}	V_{Fe}	V_{Fe}
Y_{Fe}	0	7(2*a*-6*b*)	3(2*a*-6*a*)	7(2*a*-6*a*)
Y_{6b}		0	1(2*a*-6*b*)	1(2*a*-6*b*)
V_{Fe}			0	1 (2*a*-2*a*)
V_{Fe}				0

-0.07

Table 10. Interaction of two V_{Fe}-Y_{8c}-V_{Fe} complexes

	configuration	Binding energy, eV	Configuration

a)

	Y_{8c}	Y_{8c}	V_{Fe}	V_{Fe}	V_{Fe}	V_{Fe}
Y_{8c}	0	3(8*c*-8*c*)	1(2*a*-8*c*)	1(2*a*-8*c*)	2(2*a*-8*c*)	2(2*a*-8*c*)
Y_{8c}		0	2(2*a*-8*c*)	2(2*a*-8*c*)	1(2*a*-8*c*)	1(2*a*-8*c*)
V_{Fe}			0	1 (2*a*-2*a*)	1 (2*a*-2*a*)	2 (2*a*-2*a*)
V_{Fe}				0	2 (2*a*-2*a*)	1 (2*a*-2*a*)
V_{Fe}					0	1 (2*a*-2*a*)
V_{Fe}						0

0.84

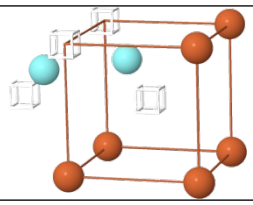

b)

	Y_{8c}	Y_{8c}	V_{Fe}	V_{Fe}	V_{Fe}	V_{Fe}
Y_{8c}	0	4(8*c*-8*c*)	1(2*a*-8*c*)	1(2*a*-8*c*)	2(2*a*-8*c*)	4(2*a*-8*c*)
Y_{8c}		0	4(2*a*-8*c*)	2(2*a*-8*c*)	1(2*a*-8*c*)	1(2*a*-8*c*)
V_{Fe}			0	1 (2*a*-2*a*)	2 (2*a*-2*a*)	4 (2*a*-2*a*)
V_{Fe}				0	1 (2*a*-2*a*)	2 (2*a*-2*a*)
V_{Fe}					0	1 (2*a*-2*a*)

-1.29

		V_{Fe}						0			
c)			Y_{8c}	Y_{8c}	V_{Fe}	V_{Fe}	V_{Fe}	V_{Fe}			
		Y_{8c}	0	5(8*c*-8*c*)	1(2*a*-8*c*)	1(2*a*-8*c*)	2(2*a*-8*c*)	5(2*a*-8*c*)			
		Y_{8c}		0	4(2*a*-8*c*)	3(2*a*-8*c*)	1(2*a*-8*c*)	1(2*a*-8*c*)			
		V_{Fe}			0	1 (2*a*-2*a*)	2 (2*a*-2*a*)	4 (2*a*-2*a*)		-1.24	
		V_{Fe}				0	1 (2*a*-2*a*)	3 (2*a*-2*a*)			
		V_{Fe}					0	1 (2*a*-2*a*)			
		V_{Fe}						0			
d)			Y_{8c}	Y_{8c}	V_{Fe}	V_{Fe}	V_{Fe}	V_{Fe}			
		Y_{8c}	0	6(8*c*-8*c*)	1(2*a*-8*c*)	1(2*a*-8*c*)	2(2*a*-8*c*)	6(2*a*-8*c*)			
		Y_{8c}		0	4(2*a*-8*c*)	4(2*a*-8*c*)	1(2*a*-8*c*)	1(2*a*-8*c*)			
		V_{Fe}			0	1 (2*a*-2*a*)	2 (2*a*-2*a*)	4 (2*a*-2*a*)		-1.37	
		V_{Fe}				0	1 (2*a*-2*a*)	5 (2*a*-2*a*)			
		V_{Fe}					0	1 (2*a*-2*a*)			
		V_{Fe}						0			

Table 11 Interaction of Y and O solutes at close distances.

	configuration								Binding energy, eV	
a)			Y_{Fe}		O_{6b}		V_{Fe}		-1.31	
	Y_{Fe}			0	2(2*a*-6*b*)		1(2*a*-2*a*)			
	O_{6b}					0	1(2*a*-6*b*)			
	V_{Fe}							0		
b)			Y_{Fe}		O_{6b}		V_{Fe}		-1.71	
	Y_{Fe}			0	4(2*a*-6*b*)		1(2*a*-2*a*)			
	O_{6b}					0	1(2*a*-6*b*)			
	V_{Fe}							0		
c)			Y_{Fe}		O_{6b}		V_{Fe}		-0.91	
	Y_{Fe}			0	3(2*a*-6*b*)		1(2*a*-2*a*)			
	O_{6b}					0	2(2*a*-6*b*)			
	V_{Fe}							0		
d)			Y_{8c}		O_{Fe}		V_{Fe}		-1.21	
	Y_{8c}			0	1(2*a*-8*c*)		1(2*a*-8*c*)			
	O_{Fe}					0	1(2*a*-2*a*)			
	V_{Fe}							0		
e)			Y_{8c}		O_{6b}		V_{Fe}	V_{Fe}	-0.01	
	Y_{8c}			0	4(8*c*-6*b*)		1(2*a*-8*c*)	1(2*a*-8*c*)		
	O_{6b}					0	6(2*a*-6*b*)	3(2*a*-6*b*)		
	V_{Fe}						0	1(2*a*-2*a*)		
	V_{Fe}							0		